

WATER HEATED HUMIDIFICATION-DEHUMIDIFICATION DESALINATION ACCOMPANYING AIR HEATING VIA EXIT BRINE

Sadam Hussain Soomro^{*1}, Imran Mir Chohan², Asif Ahmed³, Masroor Hussain⁴,
Murad Zulfiar⁵

^{*1,2,3,4}Department of Mechanical Engineering Technology, Indus University, Karachi 75300, Pakistan

⁵Department of Mechanical Engineering, Quaid-e-Awam University of Engineering, Science and Technology,
Nawabshah, 67450, Pakistan

^{*1}saddamarif7@gmail.com

DOI: <https://doi.org/10.5281/zenodo.19592474>

Keywords

Humidification Dehumidification,
Desalination, Heat-recovery,
Waste Heat, Heat exchanger

Article History

Received: 15 February 2026

Accepted: 25 March 2026

Published: 15 April 2026

Copyright @Author

Corresponding Author: *
Sadam Hussain Soomro

Abstract

The pure water shortage around the globe is worrying for human beings, therefore extraction of pure water from seawater is achieved through desalination technologies. Thermal desalination processes are many, but humidification-dehumidification (HDH) desalination is preferable because of its simplicity and usable for a small scale unit, and easily maintainable. The HDH is based on evaporation and condensation of water vapors in humidifier and dehumidifier, respectively with carrying gas like air. The energy is needed for two purposes: water vapor evaporation (the latent heat of evaporation) while another purpose is to increase the ability of air to carry away those vapors in the humidifier. The water-heated and air-heated system have higher water productivity than the bare water or air heated system alone. Therefore, in this study, modeling and thermal analysis of a water-heated HDH system along with air pre-heating (before humidifier) was achieved by utilizing the brine heat energy. The model is based on thermodynamics principles, mass, and energy conservation laws. It was found that 3.6% of energy was recovered from brine and was utilized in heating the air before humidifier, which increased the inlet air temperature and hence enhanced the evaporation, and finally, condensation was increased and that was observed with 2.6% increase in the system productivity.

1. INTRODUCTION

The population explosion and industrial development around the world continuously soar the demand for producing freshwater from saline or brackish water. Use of brackish water for agricultural needs is growing as population is increasing. The desalination is the technique to remove dissolved salts from seawater or brackish water up to the potable salinity range. Desalination technologies could be described in two types: membrane and thermal processes [1], [2], [3]. The membrane processes such as the reverse osmosis (RO) utilizes the semi permeable

membrane across the feedwater flow, while thermal processes: such as multi-stage flash (MSF), multi-effect distillation (MED), humidification-dehumidification (HDH) and other processes uses the phase change method to desalt the feedwater. The thermal systems are based on evaporation and condensation of water while membrane systems are based on the specific filter that allows the only flow of pure water while resisting the flow of dissolved minerals through it [4]. MED and MSF techniques are the most commercial thermal processes, however, they are not suitable for

smaller level units [5], [6]. RO seems to be the best method in this regard, but, RO system is highly sensitive to higher feed salt concentrations and RO requires high maintenance cost and continuous supply of electricity for its operation [7], [8], [9]. The HDH method seems to be an exciting and flexible technology that can be easily maintained and integrated with other technologies, HDH may operate at much lower temperatures as compared to other thermal methods such as MSF and MED. The main advantage of HDH is that it can operate at any low-grade waste heat energy.

The technique in HDH requires a carrier gas such as, air, carbon-dioxide or helium, but mostly air is utilized by most of the researchers, air carries away the water vapor inside the humidifier, which is then transferred to the dehumidifier for the condensing the evaporated water to get the distillate or freshwater [10], [11], [12]. Thermal energy for the carrier gas is required, more the thermal energy higher the distillate production because the capacity of the gas/air to carry the water vapor increases as the temperature of the gas/air raise [13], [14], [15]. The water vapor evaporated into the carrier gas are then recovered by bringing it in contact with cold surfaces inside the dehumidifier. This achieved by coolant water flowing inside the tubes of dehumidifier which is finned tube heat exchanger. This cooling water leaving out the dehumidifier is heated again before entering the humidifier in case of a water-heated (WH) system, while in the air-heated (AH) system the air is heated either before the humidifier or after the humidifier. Antar et al [16] experimentally investigated an AH system with single and two-stage heat recovery systems. The study suggested that using air heating along with water heating provides more productivity. Orfi et al. [17] also studied the solar HDH desalination system theoretically and experimentally. In order to boost the productivity of a system, they utilized latent heat of condensation of water vapor in the condenser to preheat the feed water. El-Agouz [18] investigated experimentally the performance of the single-stage bubble column using air bubbles passing through seawater. The results concluded that the productivity of the system rises with the

rise in water temperature and decreases in the increase in air mass flowrate. The system worked on water-heated configuration only, yet required higher temperature of water. The productivity of the system reached a maximum of 8.22 kg/h at 86 °C water temperature keeping air mass flowrate as 14 kg/h. Amer et al. [19] have also studied the only water heated (WH) cycle experimentally and theoretically in which the water flows in an open loop, whereas air circulates in a closed-loop. Their study reported maximum productivity of the system as 5.8 L/h using forced air circulation method. Sharqawy et al. [20] have studied the HDH desalination system in which comparison between the water-heated WH cycle and air-heated AH cycle was made. The study provides the best recommendations for designing any HDH system. Further, it was reported that with an increase in the maximum temperature, the value of GOR for the WH cycle reduces whereas for AH cycle its value increases. Nafey et al. [21] theoretically and experimentally conveyed the effect of operating hours per day on the productivity of the HDH unit. The results showed that when the system operated for 4 hours per day from 1:00 pm to 5:00 pm the productivity was reached 22 L/day due to the effect of solar energy storage in brackish water. Muthusamy et al. [22] conducted experimentally, the impact of various components on power consumption in the modified HDH unit. He et al. [23] studied the thermo-economic analysis of a water-heated HD desalination system powered by low-grade waste heat. Mahdizade et al. [24] proposed a novel HD desalination unit, which had a half open-air, open-water frame. After the thermodynamic simulation aiming at the novel HD desalination system, the relevant enhancement measures were also obtained at the fixed maximum temperatures. It was observed that the ambient temperature was much more important for the desalination performance, and the great advantages of the current system were also proved in the light of the gained-output-ratio (GOR) elevation. Mistry [25] concluded the entropy analysis for the open-water closed-air HDH desalination system with the air and water heaters. The mathematical models for the entropy generation and exergetic were built.

According to the simulation results, it was validated that for the entropy generation minimization it is required to determine the critical components and operating conditions, during the design of the desalination system those must be considered. A. Laknizi et al [26] utilized the brine heat recovery to heat the water coming from the dehumidifier and then the water is again heated in a feedwater heater, the parabolic trough collector was used to heat the water, and air and photovoltaic panels were utilized for water pump and fans power requirement.

Many studies reported in the literature on humidification–dehumidification (HDH) desalination systems have mainly focused on utilizing the thermal energy of the brine stream to preheat the incoming feed water before it enters the humidifier. In these conventional approaches, the heat contained in the discharged brine is recovered and transferred to the water stream in order to improve the overall thermal efficiency of the system. However, despite the importance of energy recovery in HDH systems, the possibility of using the brine heat to preheat the air stream prior to its entry into the humidifier has not been sufficiently investigated in previous research works. Therefore, the present study was carried out to explore and evaluate the potential of utilizing the available thermal energy in the brine to preheat the incoming air before it enters the humidifier section. In addition to this air preheating process, a separate water heater was also employed in the system to raise the temperature of the feed water prior to its introduction into the humidifier. By combining these two heating mechanisms, the system aims to enhance the humidification process by supplying both warmer air and warmer water to the humidifier. To analyze the performance of this configuration, a detailed HDH system model was

developed. The model was used to investigate the influence of key operating parameters, particularly the mass flow rates of air and water, on the performance characteristics of the system. Furthermore, a comparative analysis was conducted between two different configurations of the HDH system: one operating with the proposed air preheating using brine heat and the other operating without this air preheating arrangement. This comparison allowed for a clearer assessment of the impact of brine-based air preheating on the overall behavior and effectiveness of the HDH desalination system.

2. System description

The proposed HDH system consists of a dehumidifier, humidifier, heat recovery heat exchanger (HRHE), and water heat exchanger (WHE). The system is an open-air open-water (OAOW) loop Figure 1. The air is pre-heated by a brine coming from the humidifier in the heat recovery heat exchanger. The air gets heated and moist by carrying the water vapors from hot water coming at the inlet of the humidifier. The hot and humid air enters the dehumidifier to cause the condensation with feed inlet seawater [27], [28]. Some portion of the heat is recovered by feed water leaving out the dehumidifier. The condensed vapor leaves the dehumidifier as a distillate. The water is heated in a water heat exchanger (WHE) before entering the humidifier. The hot water is sprayed over packing material to enhance the evaporation rate [29], [30], [31]. The latent heat of evaporation of hot seawater is utilized by the air to carry over the water vapors. The energy for heating the water in WHE can be supplied by industrial waste, solar collector, diesel engine, process heating steam, or other forms of renewable energy. In this study process, heating steam is considered to be the energy supplier.

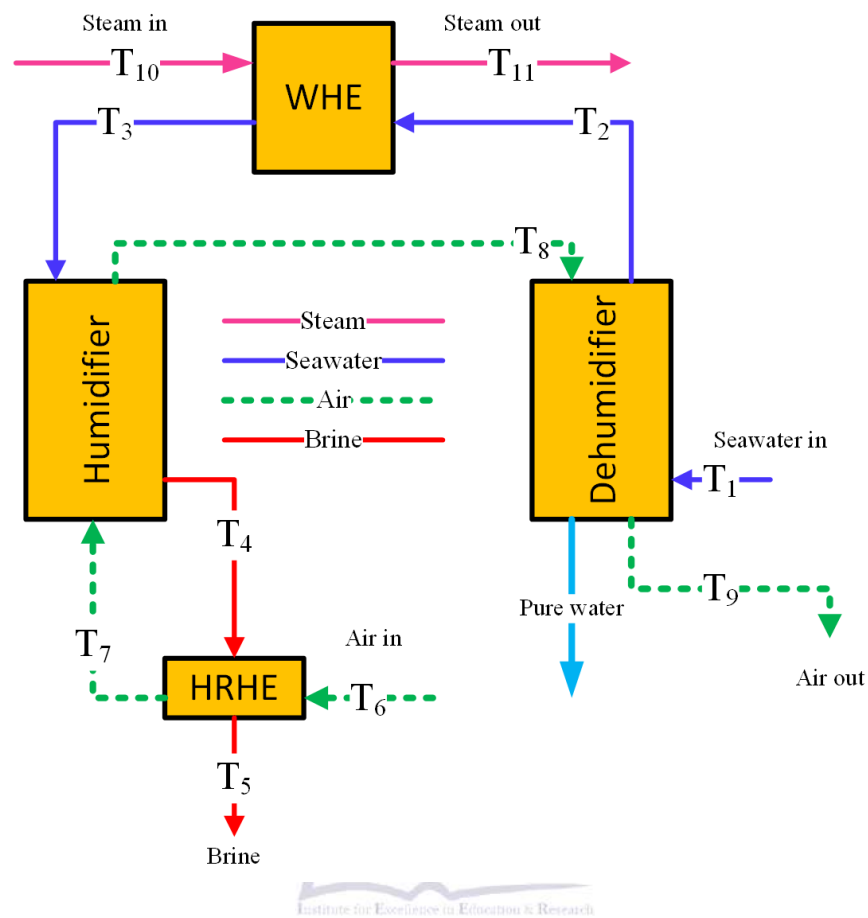


Figure.1. Schematic of proposed HDH system.

3. Mathematical Model Equations

The mathematical model for the proposed system is presented with the following key assumptions and approximations as per various literatures [8], [11], [12], [13].

- The cycle operates under steady-state conditions
- There are no heat losses from components to the surroundings, with this assumption the terms \dot{Q}_{loss} is equal to zero.
- Seawater and air inlet temperature is fixed at 25 °C
- Air at the humidifier and dehumidifier outlets is considered to be fully saturated (RH = 100%)
- Brine and air leaving the humidifier are at the same temperature
- Kinetic and potential energy terms are not included in the energy balance.
- The specific heat capacity and density of air and seawater are assumed constant at all temperatures.
- The power required for the water pump and air fan is neglected.
- The steam inlet temperature T_{10} is set to be $T_3 + 10$ °C

3.1. Humidifier

The energy balance equation for the humidification process inside humidifier is expressed as:

$$\dot{m}_a(H_{a7} - H_{a8}) = \dot{m}_{sw}H_{sw3} - \dot{m}_bH_{sw4} \quad (1)$$

where \dot{m}_a and \dot{m}_{sw} are the mass flowrates of air and seawater, respectively. H_{a7} and H_{a8} are air enthalpies at the inlet and outlet of the humidifier; H_{sw3} and H_{sw4} are seawater enthalpies at inlet and outlet of the humidifier. The saturated air the enthalpy can be calculated by the following equation provided in [32] as under:

$$H_a = 0.005853 \times T^3 - 0.497 \times T^2 + 19.87 \times T - 207.61 \quad (2)$$

The seawater enthalpy is evaluated using the coorelation provided by Sharqawy et al. [33].

$$H_{sw} = H_{pw} - S(a_1 + a_2 S + a_3 S^2 + a_4 S^3 + a_5 T + a_6 T^2 + a_7 T^3 + a_8 ST + a_9 S^2 T + a_{10} ST^2) \quad (3)$$

All coefficients used in Eq. (3) are provided in Table 1. The S is the seawater salinity and H_{pw} is the pure water enthalpy given by [22] in correlation as:

$$H_{pw} = 141.355 + 4202.07 T - 0.535 T^2 + 0.004 T^3 \quad (4)$$

Table 1. Coefficients used in finding the seawater enthalpy

a_1	-2.348×10^4	a_6	-44.17
a_2	3.15×10^5	a_7	2.139×10^{-1}
a_3	2.803×10^6	a_8	-1.997×10^4
a_4	-1.446×10^7	a_9	2.778×10^4
a_5	7.826×10^3	a_{10}	97.28

The mass balance equation within the humidifier is given by:

$$\dot{m}_b = \dot{m}_{sw} - \dot{m}_a (w_8 - w_7) \quad (5)$$

where \dot{m}_b is the brine mass flowrate, and w_8 and w_7 is the absolute humidity of the air at humidifier exit and inlet. The absolute humidity w for saturated air is a function of air temperature defined in [32] as follows:

$$w = 2.19 \times 10^{-6} T^3 - 1.85 \times 10^{-4} T^2 + 7.06 \times 10^{-3} T - 0.077 \quad (6)$$

The energy balance equation heat recovery heat exchanger (HRHE) which is used to capture some heat from the brine leaving the humidifier and add it to the air before entering the humidifier is expressed as follows:

$$\dot{m}_b c_{pb}(T_4 - T_5) = \dot{m}_a (H_{a6} - H_{a7}) \quad (7)$$

where T_4 and T_5 is the brine temperature at the humidifier outlet and HRHE outlet, respectively. The H_{a6} is the air enthalpy at HRHE inlet; H_{a7} is air enthalpy at HRHE outlet.

3.2. Dehumidifier

The energy balance equation for the dehumidifier is expressed as

$$\dot{m}_{sw}(H_{sw2} - H_{sw1}) = \dot{m}_a(H_{a8} - H_{a9}) \quad (8)$$

The H_{sw2} and H_{sw1} are seawater enthalpies at the dehumidifier outlet and inlet, while H_{a8} is air enthalpy at the dehumidifier inlet which is the same as the humidifier outlet and H_{a9} is the air enthalpy while leaving the dehumidifier.

The mass balance in the dehumidifier is defined as:

$$\dot{m}_d = \dot{m}_a (w_8 - w_9) \quad (9)$$

Where \dot{m}_d is the distillate mass flowrate which is the dependant upon wither mass flowrate of the air and difference between the absolute humidity ratios entering and leaving the dehumidifier column. The absolute humidity ratio of the air is function of air temperature.

3.3. Water heater

Water after cooling down the air and causing its condensation recovers some of the heat. Yet this water is fed into the humidifier and further heated inside the water heat exchanger (WHE). The following energy balance equation simulates the process inside the WHE:

$$\dot{m}_{sw}(H_{sw3} - H_{sw2}) = \dot{m}_s c_p (T_{10} - T_{11}) \quad (10)$$

The required areas for the two heat exchangers WHE and HRHE are calculated using the LMTD method as follows:

$$Q = U_{overall} A \text{ LMTD} \quad (11)$$

where $U_{overall}$ is the overall heat transfer coefficient, its evaluation process is described in next section.

3.3. Overall heat transfer coefficient for HRHE

The air extracts the heat from the brine coming out of the humidifier, the heat exchanger for this purpose is supposed to be a finned-tube heat exchanger in which brine flows inside the tube while air flows over the fins, the overall heat transfer is defined as

$$U_{overall} = \frac{1}{\frac{1}{\eta_f h_a A_f} + \frac{\log(r_o/r_i)}{2\pi k_t L_t} + \frac{1}{h_b A_t}} \quad (12)$$

The η_f is the fin efficiency that is almost more than 90% in every heat exchanger [34], therefore it was fixed as 90% in this study. The following C. Bougroug correlation model was used for the convective heat transfer coefficient of air [35].

$$h_a = 0.29 k_a \text{Re}_a^{0.633} \text{Pr}_a^{1/3} \text{F}^{-0.17} \quad (13)$$

$$\text{F} = \frac{SA_{fin}}{SA_{smooth}} \quad (14)$$

where F is the ratio between the surface area of the tube with fins per unit length and the tube to the surface area without fins [36].

$$SA_{fin} = \frac{A_f}{L_t} \quad (15)$$

$$SA_{smooth} = \frac{A_t}{L_t} \quad (16)$$

The waterside heat transfer coefficient was calculated by the Dittus-Boelter equation [37].

$$\text{Nu}_w = 0.023 \text{Re}^{0.8} \text{Pr}^{0.3} \quad (17)$$

3.4. overall heat transfer coefficient for WHE

The water is heated from T_2 to T_3 using the double pipe heat exchanger. The overall heat coefficient can be evaluated from Eq. (18) as follows

$$U_o = \frac{1}{\left[\frac{d_o}{d_i h_i} + \frac{d_o \ln(d_o/d_i)}{2k} + \frac{1}{h_o} \right]} \quad (18)$$

The h_i heat transfer coefficient for the seawater is calculated as described previously in section 3.3 while h_o is the heat transfer coefficient for steam: The range of convective heat transfer coefficient for the steam to liquid water for the mild steel as a material in transmission surface is in 1000–4000 W/m² C [38], therefore it is set as 1000 W/m² C in this study. The outer diameter and inner diameter of the tube are 25.4 mm and 21.1mm, respectively while mild steel has a thermal conductivity of 45 W/m C. The fouling resistance is neglected.

3.5. Gained output ratio

The HDH is thermal process and hence its efficiency is evaluated in terms of gained output ratio (GOR) defined as follows:

$$\text{GOR} = \frac{\dot{m}_d h_{fg}}{\dot{Q}_{in} + P_e} \quad (19)$$

where h_{fg} is latent heat of evaporation which is taken as 2500 kJ/kg. The term \dot{Q}_{in} is total heat provided to run the HDH system. This input also includes the P_e which is electrical power required to run the blower and

pumps for air and water flow. The value of P_e against the \dot{Q}_{in} is very very small and hence neglected in the calculation whereas \dot{Q}_{in} is calculated using following method.

$$\dot{Q}_{in} = \dot{m}_s c p_s (T_{10} - T_{11}) \tag{20}$$

The common parameter used is the L/G ratio (Liquid-to-Gas ratio) in a evaporator or condenser, also termed as mass ration (MR) which is equal to ratio of mass flowrate of seawater to the mass flowrate of air. The MR is critical metric for determining thermal performance, optimizing GOR.

4. Solution technique

The solution requires an initial estimation of T_8 to find T_7 and \dot{m}_b in order to calculate the T_5 and then the dehumidifier energy balance equation is used to find the new value of T_8 with inlet T_1 and T_2 are supposed to be 25°C and $(T_8 - 5)^\circ\text{C}$, respectively. The new T_8 is compared with the guess value and until the error is less than or equal to error (ϵ) the loop continues to run. After finding the T_8 , the original values of T_7 , T_5 and \dot{m}_b are calculated. After finding the original T_2 value

the energy required for water heating is calculated. The energy transfer rate in humidifier and dehumidifier and energy transfer in heat recovery heat exchanger is also calculated to calculate the required area of solar collector, heat exchangers for water heating, humidifier, dehumidifier, and heat recovery heat exchanger Figure 2. The code was written in MATLAB software and unknown parameters were found using the Newton Raphson method which is used to find the roots of the system of non-linear equations.

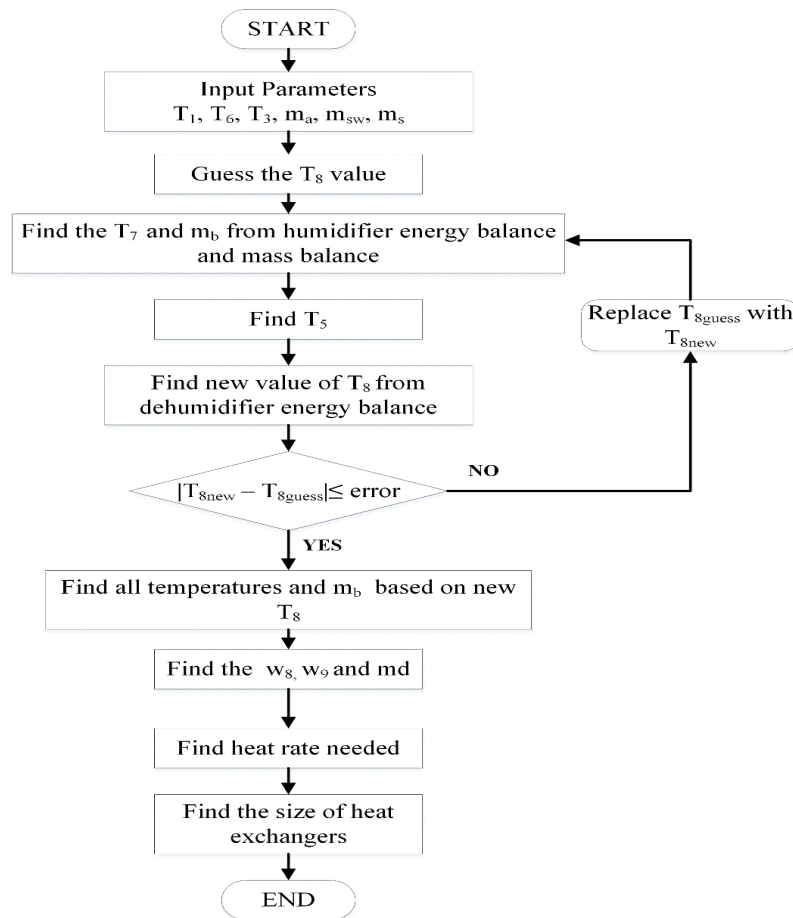


Figure. 2. Mathematical model algorithm

5. Results and discussion

The study is done for the air flowrate range in 0.4–1.0 kg/s, while the water flow rate is set in the range of 0.3–1.5 kg/s and maximum temperature within the range of 50–70°C. The maximum temperature is the seawater temperature at the humidifier inlet, the variation in air flow rate, and the maximum temperature is shown in Figure 3. The air flowrate from 0.4–0.8 kg/s makes the higher productivity and then productivity declines for a further increase in air flow rate. This happens because at an airflow rate of 0.9 kg/s and higher the air is too fast in the humidifier and passes away very quickly carrying fewer water vapors and hence lesser the water vapors in air lesser moisture available for the condensation in a dehumidifier.

The total power consumption is the heat rate utilized for heating the water in the WHE while water pump and air fan powers (P_c) are neglected in this study. The variation in thermal power consumption with maximum temperature and airflow rate is shown in Figure 4. The higher temperatures require higher energy consumptions but the productivity of the system is highly affected by airflow rate and feed water flowrate. The variation in productivity versus air and water flow rate is represented in Figure 5. As shown the higher air flowrates with higher water flowrates simultaneously increase productivity continuously. This happens because the L/G ratio (ratio of seawater flowrate and air flowrate) is such that it causes higher evaporation and higher condensation in humidifier and dehumidifier, respectively.

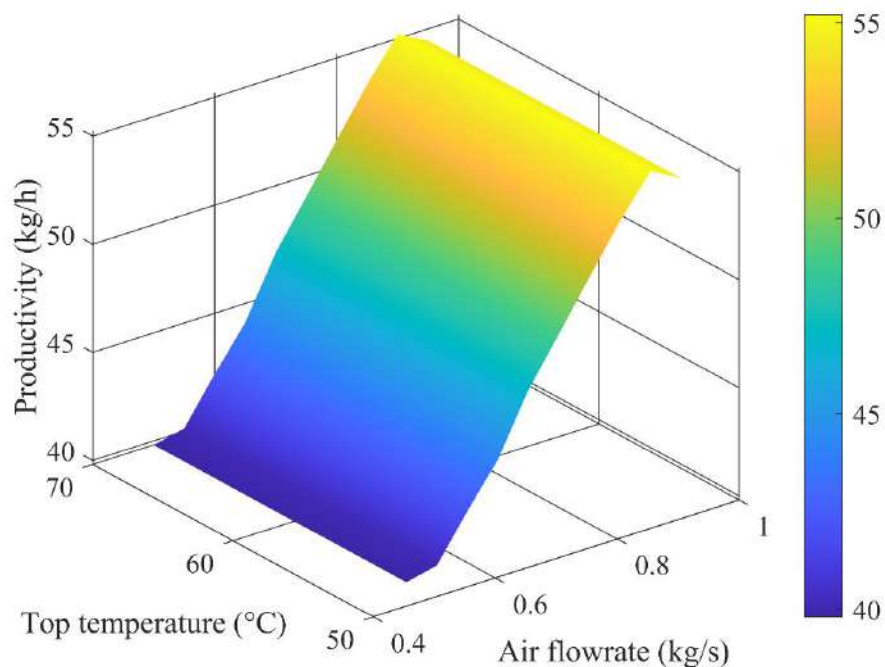


Figure.3. Productivity variation with an increase in maximum temperature (50–70°C) and an increase in the air flowrates from 0.4 to 1.0 kg/s.

The heat recovered by the inlet air from the brine causes the increase in the air humidifier inlet temperature from 25 °C up to 33.07 °C with brine temperature rise from 33.12°C to 44.54°C corresponding to the increase in the maximum

temperature from 50 °C to 70 °C shown in Figure 6. The energy recovered by the air is represented in Figure 7 which is used to pre-heat the air, the pre-heating of air is always an additional benefit to the system in order to increase the ability of air to

carry the water vapors and this results in an increase of productivity as shown in Figure 8. the

comparison is made between the productivity of the system with and without air-preheating.

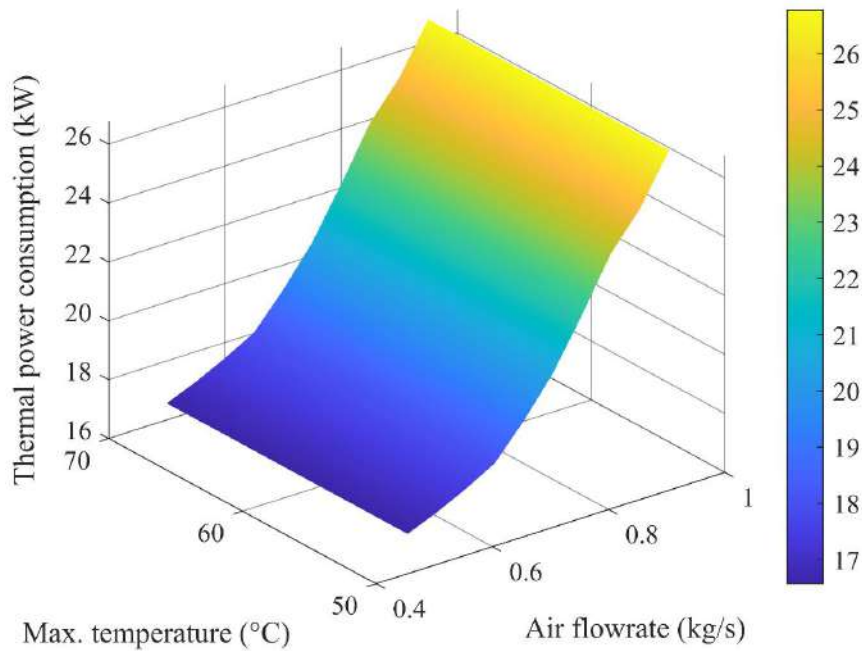


Figure.4. Total thermal power consumption vs maximum temperature and air flowrate.

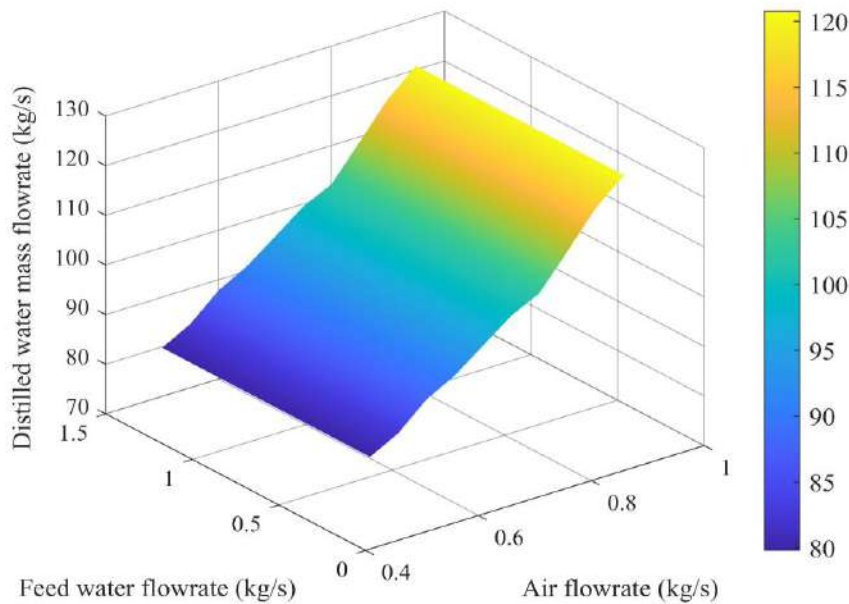


Figure.5. Impact on distilled water flow rate with variation in air and feed water flow rates.

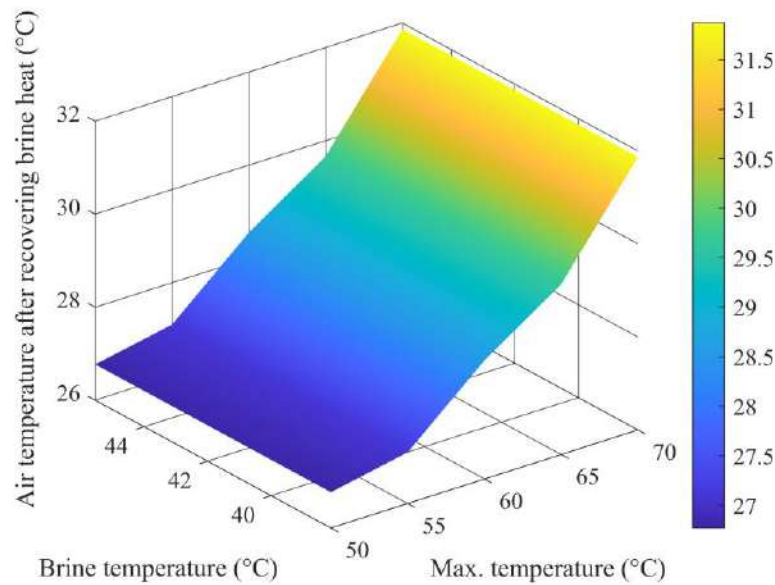


Figure.6. Air temperature increase by using brine heat energy variation with the increase in the maximum water temperature from 50 to 70°C.

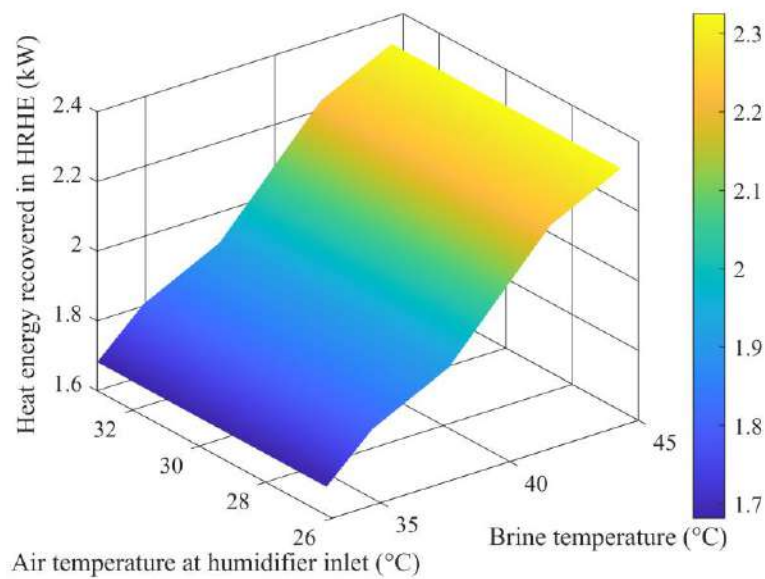


Figure.7. Heat energy rate recovered from the brine utilized to increase the air temperature from 25 to 33.07°C with an increase in brine exit temperature while the maximum temperature was increased from 50 to 70°C.

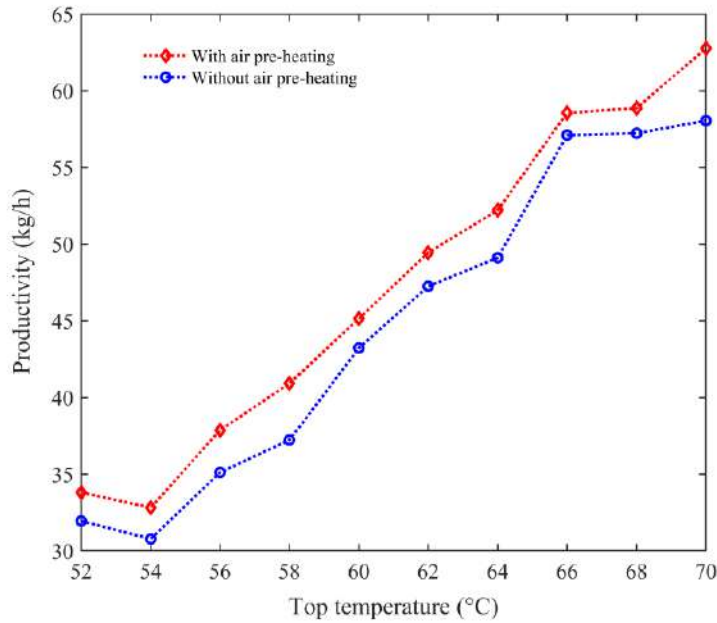


Figure.8. Productivity with and without the air pre-heating in HRHE using brine exit heat.

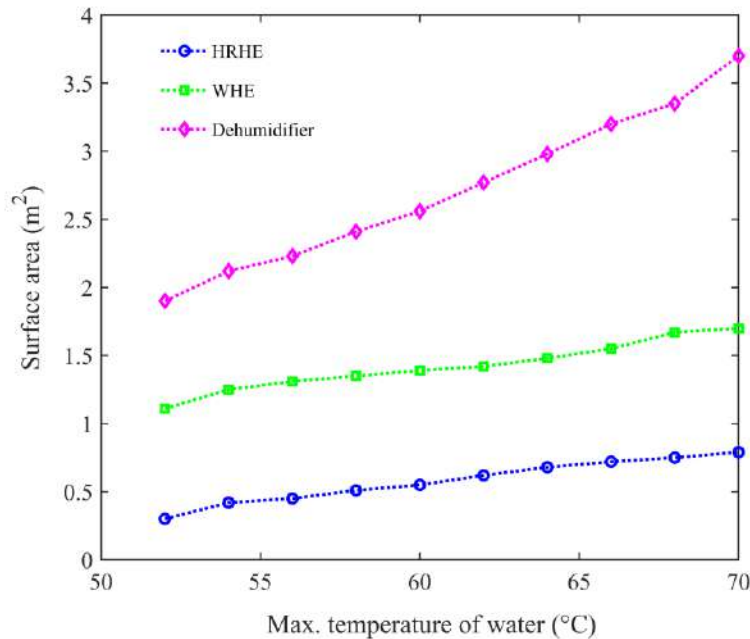


Figure.9. Surface area required for the HRHE, WHE, and dehumidifier with maximum temperature increase from 50 to 70°C.

The surface heat transfer area required for HRHE, WHE, and the dehumidifier was calculated using the LMTD method, variation of airflow rate, and maximum temperature with area required is

presented in Figure 9. The surface area required for the system increases with an increase in the maximum temperature because of the maximum temperature at the airflow rate set at 0.70 kg/s.

The increase in maximum temperature causes an increase in humidifier outlet temperature of the air which then results in more condensation rate and more heat rate which in turn requires more heat surface area. The mathematical model was

validated to confirm the accuracy and reliability of the thermodynamic model formulated. The results were validated against that of the results from Sharqawy et al. [14]. The error is less than 5% as shown in Figure 10.

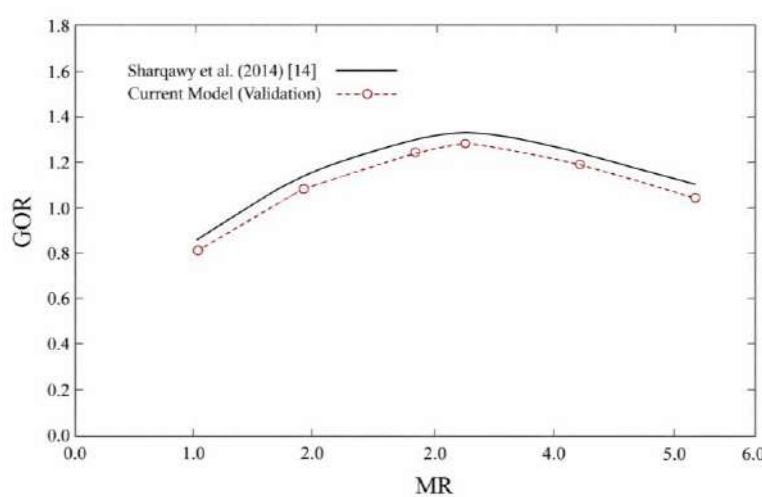


Figure.10. Comparison of the results from Sharqawy et al. [14] and current model.

6. Conclusion

In this paper, modeling and thermal analysis of an HDH unit is carried out based on energy and mass balance equations. The model equations are nonlinear and solved using the Newton Raphson method in MATLAB. The study is conducted within the air massflow rate rate of 0.4–1.0 kg/s and water mass flow rate range of 0.3–1.5 kg/s for humidifier inlet temperature (maximum temperature) of 50–70°C. The main conclusions made from this study are:

- The comparison was made between HDH systems with and without air pre-heating, it was found that about 2.6% productivity is increased with air pre-heating that was achieved using brine heat in the recovery heat exchanger of the area about 0.57 m². The temperature of inlet air was set at 25°C and was pre-heated up to 33.07°C with brine temperature rise from 33.12°C to 44.54°C corresponding to the increase in the maximum temperature from 50°C to 70°C
- The 3.6% energy was recovered during heat exchange between air and brine in the HRHE, that energy was used to pre-heat the air which in return gives about a 2.6% increase in the

production at given flowrate conditions. The HRHE tubes can get damaged with higher salinities of brine from seawater, therefore this type of system may be best suitable for desalination of brackish water or wastewater with lower salt concentration. Further, it is recommended to optimize the system for maximizing productivity and minimizing the energy use, area, and overall cost, which is the future work of this study.

Overall, it can be seen instead of wasting the brine heat into the atmosphere, it can be possible to utilize some portion of it for better overall productivity and GOR. The system is simplest form in this study, yet optimization can be made for more better performance and production.

Nomenclature

A	Heat transfer area, m ²
A_f	Fin area, m ²
A_t	Tube area, m ²
c_p	Specific heat capacity, kJ/kg°C
d_i	Inner tube diameter, m
d_o	Outer tube diameter, m
e	Enthalpy of the air, kJ/kg°C
h	Heat transfer coefficient, W/m ² °C

k	Thermal conductivity, W/m°C
L	Length, m
\dot{m}	Mass flowrate, kg/s
Nu	Nusselt number, (-)
Pr	Prandtl number, (-)
Q	Thermal power, kW
r	Radius, m
Re	Reynold's number, (-)
SA	Surface area, m ²
S	Salinity, kg/kg
T	Temperature, °C
U	Overall heat transfer coefficient, W/m ² °C
w	Absolute humidity (kg/kg)
Subscripts	
1	Seawater position at dehumidifier inlet
2	Seawater position at dehumidifier outlet
3	Seawater position at humidifier inlet
4	Brine position at humidifier outlet
5	Brine position at HRHE outlet
6	Air position at HRHE inlet
7	Air position at humidifier inlet
8	Air position at humidifier outlet, or dehumidifier inlet
9	Air position at dehumidifier outlet
10	Steam at WHE inlet
11	Steam at WHE outlet
a	Air
b	Brine
d	Distillate
i	Inner
o	Outer
t	Tube

REFERENCES

- [1] G. Amy *et al.*, "Membrane-based seawater desalination: Present and future prospects," *Desalination*, vol. 401, pp. 16-21, 2017, doi: 10.1016/j.desal.2016.10.002.
- [2] M. Ghazi, E. Essadiqi, M. Mada, M. Faqir, and A. Benabdellah, "Seawater desalination pilot plant: Optimal design and sizing of solar driven-four effect evaporators combined with heat integration analysis," *Int. Rev. Model. Simulations*, vol. 10, no. 3, pp. 177-192, 2017, doi: 10.15866/iremos.v10i3.11349.
- [3] I. M. Chohan, A. Ahmad, N. Sallih, N. Bheel, W. M. Salilew, and A. H. Almaliki, "Effect of seawater salinity, pH, and temperature on external corrosion behavior and microhardness of offshore oil and gas pipeline: RSM modelling and optimization," *Sci. Rep.*, vol. 14, no. 1, 2024, doi: 10.1038/s41598-024-67463-2.
- [4] N. Bheel *et al.*, "Optimization of durability characteristics of engineered cementitious composites combined with titanium dioxide as a nanomaterial applying RSM modelling," *Sci. Rep.*, vol. 15, no. 1, 2025, doi: 10.1038/s41598-025-94382-7.
- [5] G. P. Narayan, M. H. Sharqawy, J. H. Lienhard V, and S. M. Zubair, "Thermodynamic analysis of humidification dehumidification desalination cycles," *Desalin. Water Treat.*, vol. 16, no. 1-3, pp. 339-353, 2010, doi: 10.5004/dwt.2010.1078.
- [6] N. Bheel *et al.*, "Synergistic effect of recycling waste coconut shell ash, metakaolin, and calcined clay as supplementary cementitious material on hardened properties and embodied carbon of high strength concrete," *Case Stud. Constr. Mater.*, vol. 20, 2024, doi: 10.1016/j.cscm.2024.e02980.
- [7] A. Altaee, J. Zhou, A. Alhathal Alanezi, and G. Zaragoza, "Pressure retarded osmosis process for power generation: Feasibility, energy balance and controlling parameters," *Appl. Energy*, vol. 206, pp. 303-311, 2017, doi: 10.1016/j.apenergy.2017.08.195.

- [8] W. Luo *et al.*, "Osmotic versus conventional membrane bioreactors integrated with reverse osmosis for water reuse: Biological stability, membrane fouling, and contaminant removal," *Water Res.*, vol. 109, pp. 122–134, 2017, doi: 10.1016/j.watres.2016.11.036.
- [9] N. Bheel, I. M. Chohan, M. Alwetaishi, S. A. Waheeb, and L. Alkhatabi, "Sustainability assessment and mechanical characteristics of high strength concrete blended with marble dust powder and wheat straw ash as cementitious materials by using RSM modelling," *Sustain. Chem. Pharm.*, vol. 39, 2024, doi: 10.1016/j.scp.2024.101606.
- [10] A. Giwa, "Salty groundwater treatment: Recovery of magnetic nano-particles," *Int. Conf. Hydrol. Groundw. expo*, 2013.
- [11] C. Link, "The potential of solar-driven humidification-dehumidification desalination for small-scale decentralized water production," no. 4, pp. 1187–1201, 2012.
- [12] K. Bourouni, M. T. Chaibi, and L. Tadrif, "Water desalination by humidification and dehumidification of air: State of the art," *Desalination*, vol. 137, no. 1–3, pp. 167–176, 2001, doi: 10.1016/S0011-9164(01)00215-6.
- [13] M. H. Hamed, A. E. Kabeel, Z. M. Omara, and S. W. Sharshir, "Mathematical and experimental investigation of a solar humidification-dehumidification desalination unit," *Desalination*, vol. 358, pp. 9–17, 2015, doi: 10.1016/j.desal.2014.12.005.
- [14] I. M. Chohan, A. Ahmad, N. Bheel, T. Najeh, and A. H. Almaliki, "Sustainability assessment of different pipeline materials in freshwater supply systems," *Front. Mater.*, vol. 12, 2025, doi: 10.3389/fmats.2025.1566151.
- [15] S. Kumar, H. Sakidin, M. Zafar, H. B. Lanjwani, and I. M. Chohan, "Nanofluid Thermophysical Property Modeling for Enhanced Oil Recovery: A Comprehensive Review and Future Outlook for Artificial Intelligence Integration," *Arch. Comput. Methods Eng.*, 2025, doi: 10.1007/s11831-025-10329-1.
- [16] M. A. Antar and M. H. Sharqawy, "Experimental investigations on the performance of an air heated humidification-dehumidification desalination system," *Desalin. Water Treat.*, vol. 51, no. 4–6, pp. 837–843, 2013, doi: 10.1080/19443994.2012.714598.
- [17] J. Orfi *et al.*, "Experimental and theoretical study of a humidification-dehumidification water desalination system using solar energy," *Desalination*, vol. 168, no. 1–3, pp. 151–159, 2004, doi: 10.1016/j.desal.2004.06.181.
- [18] S. A. El-Agouz, "A new process of desalination by air passing through seawater based on humidification-dehumidification process," *Energy*, vol. 35, no. 12, pp. 5108–5114, 2010, doi: 10.1016/j.energy.2010.08.005.
- [19] E. H. Amer, H. Kotb, G. H. Mostafa, and A. R. El-Ghalban, "Theoretical and experimental investigation of humidification-dehumidification desalination unit," *Desalination*, vol. 249, no. 3, pp. 949–959, 2009, doi: 10.1016/j.desal.2009.06.063.
- [20] M. H. Sharqawy, M. A. Antar, S. M. Zubair, and A. M. Elbashir, "Optimum thermal design of humidification dehumidification desalination systems," *Desalination*, vol. 349, pp. 10–21, 2014, doi: 10.1016/j.desal.2014.06.016.
- [21] A. S. Nafey, H. E. S. Fath, S. O. El-Helaby, and A. M. Soliman, "Solar desalination using humidification dehumidification processes. Part I. A numerical investigation," *Energy Convers. Manag.*, vol. 45, no. 7–8, pp. 1243–1261, 2004, doi: 10.1016/S0196-8904(03)00151-1.

- [22] C. Muthusamy and K. Srithar, "Energy saving potential in humidification-dehumidification desalination system," *Energy*, vol. 118, pp. 729-741, 2017, doi: 10.1016/j.energy.2016.10.098.
- [23] W. F. He, D. Han, W. P. Zhu, and C. Ji, "Thermo-economic analysis of a water-heated humidification-dehumidification desalination system with waste heat recovery," *Energy Convers. Manag.*, vol. 160, pp. 182-190, 2018, doi: 10.1016/j.enconman.2018.01.048.
- [24] E. Z. Mahdizade and M. Ameri, "Thermodynamic investigation of a semi-open air, humidification dehumidification desalination system using air and water heaters," *Desalination*, vol. 428, pp. 182-198, 2018, doi: 10.1016/j.desal.2017.11.032.
- [25] K. H. Mistry, J. H. Lienhard, and S. M. Zubair, "Effect of entropy generation on the performance of humidification-dehumidification desalination cycles," *Int. J. Therm. Sci.*, vol. 49, no. 9, pp. 1837-1847, 2010, doi: 10.1016/j.ijthermalsci.2010.05.002.
- [26] A. Lakhani *et al.*, "Modeling and thermal analysis of small scale desalination system using humidification- dehumidification process driven by solar energy," *Proc. 2018 6th Int. Renew. Sustain. Energy Conf. IRSEC 2018*, 2018, doi: 10.1109/IRSEC.2018.8702981.
- [27] I. MIR, S. SAMO, T. HUSSAIN, I. ALI, and H. A. K. DURANI, "Influence of Convergent Section Length and Angle on Performance of Supersonic Nozzle," *Sindh Univ. Res. J. -Science Ser.*, vol. 49, no. 004, pp. 727-732, 2017, doi: 10.26692/surj/2017.12.48.
- [28] M. C. Rozina Chohan, Imran Mir Chohan, "Comparative Analysis of Different Convergent Section Angles and Working Fluids on Supersonic Nozzle Thrust Force by Computational Fluid Dynamic (CFD)," *Tech. J.*, vol. Vol 30, no. 02, 2025.
- [29] I. M. Chohan, A. Ahmad, N. Sallih, N. Bheel, and A. H. Almaliki, "Effect of seawater salinity and temperature on material performance and marine ecotoxicity of offshore pipeline using RSM modelling," *Int. J. Environ. Sci. Technol.*, vol. 23, no. 2, 2026, doi: 10.1007/s13762-025-06869-5.
- [30] I. Mir Chohan *et al.*, "Corrosion Behaviour and Microhardness of ASTM 106 Grade B Carbon Steel Offshore Pipeline at Different Locations in Malaysia," *J. Adv. Res. Micro Nano Eng. J. homepage*, vol. 38, pp. 1-11, 2025, [Online]. Available: https://semarakilmu.com.my/journals/index.php/micro_nano_engineering/index
- [31] I. M. Chohan, A. Ahmad, N. Sallih, N. Bheel, and A. Almaliki, "Correction: Effect of seawater salinity and temperature on material performance and marine ecotoxicity of offshore pipeline using RSM modelling," *Int. J. Environ. Sci. Technol.*, vol. 23, no. 3, 2026, doi: 10.1007/s13762-025-07011-1.
- [32] M. M. Farid, S. Parekh, J. R. Selman, and S. Al-Hallaj, "Solar desalination with a humidification-dehumidification cycle: Mathematical modeling of the unit," *Desalination*, vol. 151, no. 2, pp. 153-164, 2003, doi: 10.1016/S0011-9164(02)00994-3.
- [33] M. H. Sharqawy, J. H. Lienhard V, and S. M. Zubair, "Thermophysical properties of seawater: A review of existing correlations and data," *Desalin. Water Treat.*, vol. 16, no. 1-3, pp. 354-380, 2010, doi: 10.5004/dwt.2010.1079.
- [34] Y. Cengel, "Heat and mass transfer: fundamentals and applications," 2014.
- [35] M. Ameri and M. SeydEshaghi, "A novel configuration of reverse osmosis, humidification-dehumidification and flat plate collector: Modeling and exergy analysis," *Appl. Therm. Eng.*, vol. 103, pp. 855-873, 2016, doi: 10.1016/j.applthermaleng.2016.04.047.

- [36] I. Abdallah, "Cost effective treatment of produced water using co-produced energy sources," *Proc. -SPE Annu. Tech. Conf. Exhib.*, vol. 7, pp. 5612-5620, 2014, doi: 10.2118/173475-stu.
- [37] G. E. Miller, "Optimum fin spacing for heat transfer per unit length of heat exchange section," 1967.
- [38] A. P. S Kakaç, H Liu, *Heat exchangers: selection, rating, and thermal design*, vol. 36, no. 01. 1998. doi: 10.5860/choice.36-0348.

